

## PREDICTION OF THE ELECTRIC POWER BY OSCILLATING WATER COLUMN WAVE POWER PLANTS ON BAWEAN ISLAND USING LSTM

**Risma Madurahma Putri** \*, **Luthfi Hakim** , **Dian C Rini Novitasari** ,  
**Ahmad Hanif Asyhar** , **Fajar Setiawan** 

<sup>1,2,3,4</sup> *Mathematics Department, Faculty of Science and Technology, UIN Sunan Ampel Surabaya  
Jln. Ahmad Yani, No. 117, Jemur Wonosari, Kecamatan Wonocolo, Surabaya, 60237, Indonesia*

<sup>5</sup>*Perak Maritime Meteorology Station II  
Jln. New Kalimas, No. 97B, Perak Utara, Pabean Cantikan, Surabaya, 60165, Indonesia*

*Corresponding author's e-mail: \* [madurahmalearning@gmail.com](mailto:madurahmalearning@gmail.com)*

### ABSTRACT

#### Article History:

Received: 29<sup>th</sup> October 2024  
Revised: 5<sup>th</sup> February 2025  
Accepted: 27<sup>th</sup> May 2025  
Available online: 1<sup>st</sup> September 2025

#### Keywords:

Bawean Island;  
Electrical Energy;  
Long Short Term Memory;  
Oscillating Water Column;  
Wave Power Plant.

The demand for electricity in Indonesia continues to increase in line with population growth and the expansion of economic development. This increase is not matched by the diminishing electricity resources, as fossil fuels, which are non-renewable, are being used. Therefore, there is a need for renewable energy sources that can be utilized as long-term electricity resources. The abundant marine areas in Indonesia make it a potential source of alternative energy, one form of its utilization is the Ocean Wave Power Plant using the Oscillating Water Column (OWC) method. Bawean Island in Gresik is one of the regions that has this potential, while also facing long-standing electricity supply limitations that have resulted in uneven electricity distribution among the community. The problem does not stop at power generation but also extends to the transmission system between supply and demand. This research is conducted to predict the electricity generated by the ocean wave power plant to help avoid mismatches when supplying electricity. This study uses time series data from January 1st, 2021, to May 5th, 2024, which includes wave height, length, period, and amplitude. Electricity prediction based on these parameters can be performed using deep learning-based methods that can effectively process sequential time series data, such as the Long Short Term Memory (LSTM) method, by experimenting with the number of neurons, epochs, and batch sizes. The best prediction results for the variables of height, length, period, and amplitude of the waves obtained MAPE values of 0.3657%, 0.1637%, 0.0888%, and 0.3480%, respectively. The electricity prediction results from the best parameters obtained a MAPE of 0.3549%.



This article is an open access article distributed under the terms and conditions of the [Creative Commons Attribution-ShareAlike 4.0 International License](https://creativecommons.org/licenses/by-sa/4.0/) (<https://creativecommons.org/licenses/by-sa/4.0/>).

#### How to cite this article:

R. M. Putri, L. Hakim, D. C. R. Novitasari, A. H. Asyhar and F. Setiawan., "PREDICTION OF THE ELECTRIC POWER BY OSCILLATING WATER COLUMN WAVE POWER PLANTS ON BAWEAN ISLAND USING LSTM," *BAREKENG: J. Math. & App.*, vol. 19, no. 4, pp. 2287-2300, December, 2025.

Copyright © 2025 Author(s)

Journal homepage: <https://ojs3.unpatti.ac.id/index.php/barekeng/>

Journal e-mail: [barekeng.math@yahoo.com](mailto:barekeng.math@yahoo.com); [barekeng.journal@mail.unpatti.ac.id](mailto:barekeng.journal@mail.unpatti.ac.id)

Research Article • Open Access

## 1. INTRODUCTION

Indonesia requires electricity and fossil fuels as the population increases, development and economic expansion every year. This non-renewable resource derived from fossils supplies most of global energy needs to date. However, the real threat of energy reserves which are decreasing day by day and the cycle of formation which takes millions of years, means that these resources cannot meet human needs for a long time in the future [1]. To meet energy needs in the long term, various problems can arise. Data collected in 2012 shows that non-renewable energy in the form of gas, oil and coal contributed 20.6% of the largest energy supply in Indonesia [2]. On the other hand, the realization of Indonesia's national resilience depends, in part, on meeting energy needs. Any disruption or shortage of energy supply will have a direct impact on the country's economic growth and development. Apart from the threat of energy scarcity, the negative impact of fossil fuels plays a major role in the global climate crisis, making it very important to commit to reducing the emissions released into the surrounding environment. The energy transition, which reduces dependence on non-renewable energy, is part of avoiding emissions towards cleaner energy. In the Electricity Procurement Plan for 2018-2027, the target is to increase the portion of new-renewable energy as the main energy source for electricity generation to 23% in 2025 [3]. Until now, efforts to divert electricity sources to new-renewable energy continue to be made, one of which is by utilizing Indonesia's abundant natural potential such as the sea. Therefore, the implementation of ocean wave power plant is essential as a renewable energy source.

Indonesia as a maritime and country has enormous marine energy potential. The continuous and never-ending existence of sea water can be used as an alternative energy source to overcome dependence on unclean energy sources in the future [2]. Ocean waves, with abundant energy every day, are one source of energy that has not been widely utilized [4]. Sea waves are created from generating power originating from objects moving around the sea surface, seismic disturbances, and others [5]. In general, the frequency of wind that occurs in certain zones throughout the year influences wave characteristics [6]. Wind speed, time and distance are three factors that influence waves. If wind speed increases, the size and length of ocean waves will also increase over time [7]. Oscillating Water Column (OWC) is one way of Wave Energy Converter (WEC) to convert ocean wave energy into electrical energy [1].

Various studies have been carried out on the opportunities for converting ocean wave energy into a source of electrical energy using the OWC method, one of which is on Bawean Gresik Island. Until now, the demand for electrical energy on Bawean Island is supplied by the Diesel Power Plant, however there are still several areas that have not been touched by electricity. Another problem often experienced by Bawean Island Diesel Power Plant is delays in the delivery of diesel fuel due to large waves which hinder ship navigation. Therefore, it is necessary to use renewable energy to support electricity needs on Bawean Island. Looking at the topography of Bawean Island which has quite high sea waves, it can be said that the waters of Bawean Island have the potential to produce a clean energy source ocean wave power plant with the OWC type [8]. Energy supplier problems don't just stop there, but continues to be the transmission between supply and demand. A mismatch in transmitting the electrical power supplied with the electrical power that the community needs can become a new problem. The mismatch can be in the form of a shortage or excess when supplying electrical energy, which can result in problems such as a decrease in electric current, blackouts, damage to electrical devices, waste of energy, and others [9]. To prevent this from happening, accurate calculations and forecasts are needed to determine the amount of electrical power that can be generated by the ocean wave power plant. So that it can then be adjustments to the amount of electrical power distributed to the community and the amount stored as reserves [10].

Wave height, wave period, wave length, wave amplitude, and dimensions of the OWC column are some important factors whose seasonal trends can influence how optimally a wave power plant can generate electrical power [1]. Furthermore, the accurate prediction of electrical power occupies an important position in energy reliability and performance, impacting the cost and the entire energy management system [11]. Several previous studies have predicted the electrical power by oscillating water column method, one of which was conducted in Banyuwangi using Extreme Learning Machine (ELM) and achieved an evaluation MAPE of 2.3367% [10]. There are many methods that can provide better performance developed for forecasting research, one of which is Long Short Term Memory (LSTM). Example of research that predicts rainfall by comparing ELM, LSTM, Holt-Winters, RNN Relu, RNN Silu and ARIMA, resulting in LSTM as the best method with an accuracy of 88% and the smallest RMSE of 0.33 in the comparison epoch the same, namely 40 [12]. Another implementation in research that uses PCA and LSTM to predict daily rainfall, produces a MAPE of 0.0018 with a total hidden 100, batch size 32, and learn rate drop period 50 [13].

Subsequent research that predicted the development of COVID-19 cases in Telangana, obtained LSTM results that outperformed ARIMA, MLP, and ELM and LSTM with RMSE of 71.12 compared to ARIMA (258.20), ELM (553.67) and MLP (641.86) [14].

Based on the issues outlined previously, this study is focusing on the wave energy potential of Bawean Island and Long Short Term Memory (LSTM) has a strong capability for forecasting, this research will apply the LSTM method to predict the amount of electrical power produced by ocean wave power plant using OWC. It is hoped that the application of LSTM can provide good prediction results to supporting the more efficient utilization of clean energy and minimize problems when transmitting electrical energy to the community in the future.

## 2. RESEARCH METHODS

### 2.1 Research Data

Bawean Island is located in Gresik Regency, East Java Province and consists of Sangkapura District and Tambak District. Geographically, Bawean Island is approximately 120 kilometers north of the city of Surabaya, and has an area of around 196.97 Km<sup>2</sup> [8]. The location of this research in Tambak District at coordinates 112°69'48.39" East Longitude and 5°71'88.28" South Latitude as shown in **Figure 1**.

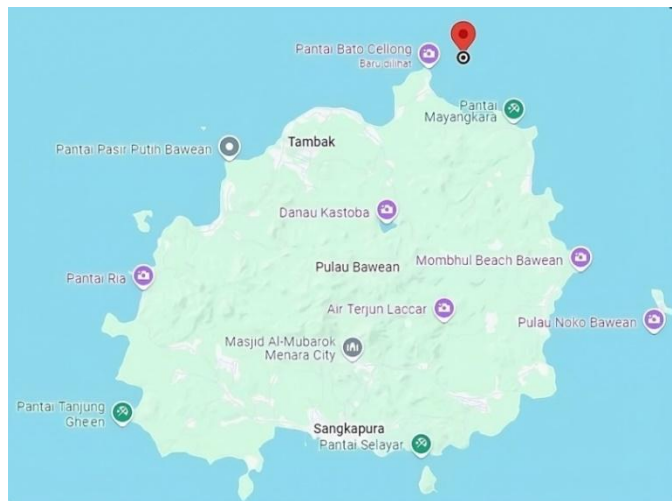


**Figure 1. The Coordinate Point of Location Research.**

Source : [15]

Based on **Figure 1**, this location research is about 1.87 Km from Bato Cellong Beach. This research data for this study are quantitative data obtained directly from the Perak Maritime Meteorology Station II, such as data on wave height, wave period, wave length and wave amplitude from January 1st, 2021 to May 5th, 2024. The dataset obtained are time series recorded of half daily, as shown in **Table 1**.

**Table 1. Half Daily Sea Wave Dataset**

Date time	Wave height (m)	Wave period (s)	Wave length (m)	Wave amplitude (m)
2021-01-01 00:00:00	0.92	4.59	35.07	1.21
2021-01-01 12:00:00	0.94	4.32	31.62	1.23
2021-01-02 00:00:00	0.88	4.10	28.14	1.16
:	:	:	:	:
2024-05-04 12:00:00	0.41	3.99	26.14	0.68
2024-05-05 00:00:00	0.57	3.24	17.35	0.95

Waves have several parameters, including height, period, length, and amplitude. The height of a wave is the perpendicular distance between the crest and the trough of the wave. The period of a wave is the time taken between two crests at the same point. The wavelength is the horizontal distance between two

consecutive crests. The amplitude of a wave is the maximum displacement of the wave's peak [16]. The wave height suitable for Wave Energy Converters (WEC) using the Oscillating Water Column (OWC) method varies depending on the design and technical specifications of the device. Generally, waves with a height of approximately 1 meter are considered capable of producing energy efficiently [17]. In this research data, the average wave height is 0.9716 meters.

## 2.2 Technical Research

The steps of this research are preprocessing, analysis, and evaluation as visualized in **Figure 2**.

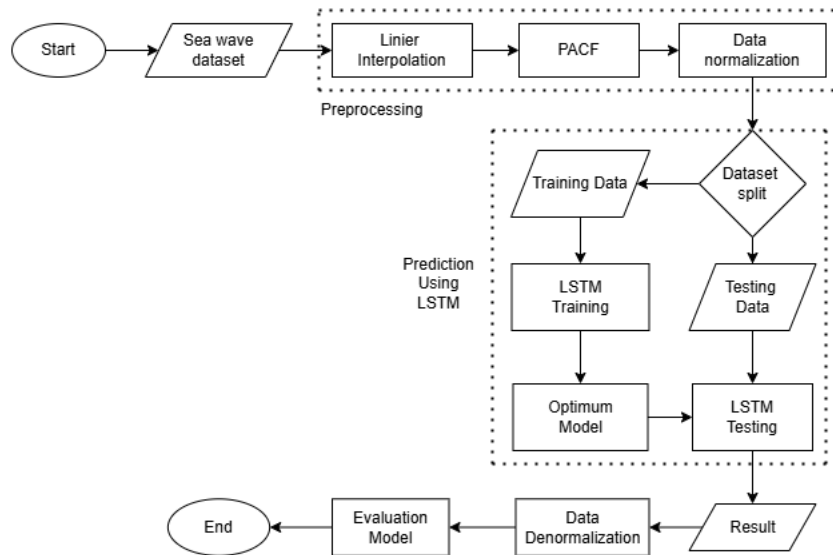


**Figure 2. Research Flow Chart**

The research flowchart is structured as following **Figure 2**. First, gather the data, then perform data preprocessing by filling in missing values using linear interpolation, calculating daily averages, and determining the lag values for each variable on the PACF plot. After that, normalize the data using Min-Max Scaler and establish the sequential time series pattern. The next step is split the data, allocating 80% for training data and 20% for testing data. The use of this split dataset ratio preserves the order of the data, so it is closer to the real conditions. The training data is used to develop the best LSTM model, which is then utilized for making predictions using the testing data. Next, perform denormalization to revert the predicted values back to their original values. Finally, MAPE will evaluate the LSTM model.

## 2.3 Ocean Wave Power Plant-Oscillating Water Column (OWC)

Ocean wave power plant works by exploiting the rise and fall of ocean waves and pitching of waves [18]. Ocean wave power plants are divided into four types, including OWC, AWS (Archimedes Wave Swing), Pelamis, and Duck. Among the four, OWC is the type of ocean wave power plant most studied by many researchers. The simplicity of the OWC system is the main point that makes OWC superior compared to wave energy conversion others [19]. The simplicity of the OWC construction system lies in the simplicity of the main components, namely two components in the form of Air Chamber and Air Turbine Generator. This system generates electricity by involving vertical pipes that allow water to rise and fall due to sea waves [20]. This movement creates air pressure that flows in and out of the hole at the top of the column and rotates the turbine continuously. This continuous rotation of the turbine produces mechanical power for the system, which then activates the generator [21]. There are two types of installation locations for the ocean wave power plant system, namely beach-based and offshore. The Offshore System is constructed with a coil mechanism at a depth of 40 meters that uses wave movement to pump the turbine. Meanwhile, the system is beach based generally consists of a channel system, a float system, and an oscillating water column system [22].

The conversion of wave motion energy into air pressure potential energy is influenced by several things, including wave height and chamber area. The larger the size or area of the chamber, the greater the electrical energy produced [23]. The calculation of the amount of electrical power produced by ocean wave power plant OWC is formulated in **Equation (1)** [24].

$$P_w = \frac{E_w}{T} = \frac{\frac{1}{4} \rho g w a^2 \lambda}{T} \quad (1)$$

Where  $P_w$  is electrical power (watts),  $\rho$  is the density of water (1030 Kg/m<sup>3</sup>),  $g$  is the earth's gravitational force (9.81 m/s<sup>2</sup>),  $w$  is broad chamber (m<sup>2</sup>),  $a$  is the wave amplitude (m),  $\lambda$  is the wave length (m), and  $T$  is the wave period (second).

## 2.4 Linier Interpolation

Interpolation is a method for determining values between two ranges based on a specific mathematical function. In linear interpolation, two values that have a linear relationship can be connected so that the point between them can be determined to have a value [25]. Linear interpolation is used to find missing data values between a known number of data points. The formula is shown in **Equation (2)** [26].

$$x = \left( \frac{y - y_0}{y_1 - y_0} \right) (x_1 - x_0) + x_0 \quad (2)$$

## 2.5 Min-max Scaler Normalization

Min-Max Scaler normalization is a normalization that works by changing the scale of the original value to a scale of 1 for the top edge and 0 for the bottom edge of [0,1] without replacing data information through linear transformation on the original data [27]. Normalization creates a balance in the comparative values among data, leading to a simplification of features as a solution to the issue of original feature values being too disparate. The formula is shown in **Equation (3)** [28].

$$X_{norm} = \frac{X - X_{min}}{X_{max} - X_{min}} \quad (3)$$

## 2.6 Long Short Term Memory (LSTM)

Long Short Term Memory (LSTM) is a method that produces predictions based on information that has been stored for a long period of time [29]. LSTM is a modification of the method Recurrent Neural Network (RNN) which is specifically designed to handle sequential data [30]. To create sequential data, a partial correlation function is needed between the current observation and previous observations, namely the PACF vector (Partial Autocorrelation Function) [31].

Although the special characteristic of RNN is that it uses input sequential data, however, is a problem vanishing and exploding gradient in RNN can appear when values change from one layer to the next layer in the architecture. This long-term dependency problem can be solved by the LSTM method, which provides memory gates to the hidden layer cells. Therefore, LSTM can learn long patterns from sequential data to prevent the situation of vanishing gradients [32]. The basic unit of LSTM is called a memory cell where each cell has a linear unit with constant weight [33]. In the LSTM architecture there are 3 gates, the LSTM architecture is visualized in **Figure 3**.

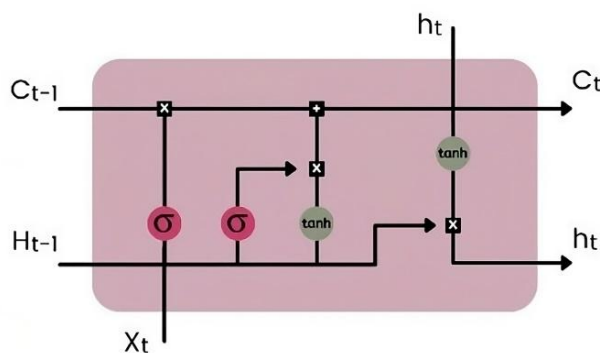


**Figure 3.** Long Short Term Memory Architecture.

Following are the functions and formulas of each gate [34]:

The First Gate is forget gate, plays a role in determining what information should be passed on or what should be discarded. Forget gate formulated in **Equation (4)**.

$$f_t = \sigma (W_f \cdot [X_t, h_{t-1}] + b_f) \quad (4)$$

Where  $f_t$  is forget gate,  $\sigma$  is a sigmoid function,  $W_f$  is the weight forget gate,  $X_t$  is the latest timestep,  $h_{t-1}$  is output timestep 1, and  $b_f$  is the bias weight forget gate.

The Second Gate is input gate, plays a role in determining what information will be used new knowledge and saved. In this gate, there are two activation functions, namely sigmoid and tanh. Input gate and new knowledge formulated in **Equation (5)** and **Equation (6)**.

$$i_t = \sigma (W_i \cdot [X_t, h_{t-1}] + b_i) \quad (5)$$

$$\tilde{C}_t = \sigma (W_c \cdot [X_t, h_{t-1}] + b_c) \quad (6)$$

Where  $i_t$  is input gate,  $W_i$  is the weight input gate,  $b_i$  is the bias weight input gate,  $\tilde{C}_t$  is a new candidate cell state,  $W_c$  is the weight cell state, and  $b_c$  is the bias weight cell state. Furthermore,  $i_t$  and  $\tilde{C}_t$  will be used to set cell state the new one. Cell state formulated in **Equation (7)**.

$$C_t = f_t \cdot C_{t-1} + i_t \cdot \tilde{C}_t \quad (7)$$

Where  $C_t$  is cell state,  $f_t$  is forget state,  $C_{t-1}$  is cell state timestep 1, and  $i_t$  is input state.

The Third Gate is output gate, functions to produce output from calculations that have been run. Output gate formulated in **Equation (8)**.

$$O_t = \sigma (W_o \cdot [X_t, h_{t-1}] + b_o) \quad (8)$$

Where  $O_t$  is output gate,  $W_o$  is the weight output gate, and  $b_o$  is the bias weight output gate.

## 2.7 Data Denormalization

Denormalization is the process of reverting data that has been normalized back to its original size. This process is carried out to restore the range of predicted values to their original range, allowing for evaluation using MAPE to be conducted [35].

## 2.8 Mean Absolute Percentage Error (MAPE)

After the training and testing process is complete, accuracy testing is carried out by comparing the prediction results with actual data using MAPE formulated in **Equation (9)** [36].

$$MAPE = \frac{\sum_{i=1}^n \left| \frac{y_i - \hat{y}_i}{y_i} \right| \times 100\%}{n} \quad (9)$$

Where  $y_i$  is the actual value,  $\hat{y}_i$  is the predicted value, and  $n$  is the number of data points. Good prediction results are shown by small MAPE values. The MAPE value criteria are shown in **Table 2**, a larger MAPE value indicates worse model performance, as it reflects a greater deviation between predicted and actual values. Conversely, a smaller MAPE value suggests better model performance, indicating a lower discrepancy between predictions and actual outcomes.

**Table 2. Criteria of MAPE**

MAPE	Criteria
<10%	The prediction result are very good
10-20%	The prediction result are good
20-50%	Prediction result are feasible/adequate
>50%	Bad prediction result

### 3. RESULTS AND DISCUSSION

#### 3.1 Result of Data Preprocessing and PACF Plot

The half daily sea wave dataset in **Table 1** has a total of 16 missing data points, which were filled in using the linear interpolation method. The descriptive statistic has been presented in **Table 3**. After fill the missing data points, a daily average was calculated to obtain daily time series data, resulting in a total of 1222 data points. This daily data will be used as the input for the research, as indicated in **Table 4**.

**Table 3. Descriptive Statistic and Missing Data**

Variable	Count	Min	Mean	Max	Total Missing	Missing (%)
<b>Date time</b>	2443	-	-	-	0	0%
<b>Wave height (m)</b>	2443	0.02	0.97	3.69	16	0.66%
<b>Wave period (s)</b>	2443	2.22	4.06	7.12	16	0.66%
<b>Wave length (m)</b>	2443	8.17	28.23	89.81	16	0.66%
<b>Wave amplitude (m)</b>	2443	0.01	0.91	4.85	16	0.66%

**Table 4. Daily Sea Wave Dataset**

Date time	Wave height (m)	Wave period (s)	Wave length (m)	Wave amplitude (m)
2021-01-01	0.930	4.455	33.345	1.220
2021-01-02	0.895	4.920	25.790	1.180
2021-01-03	0.775	4.190	29.685	1.015
:	:	:	:	:
2024-05-04	0.415	3.985	26.245	0.690
2024-05-05	0.570	3.240	17.350	0.950

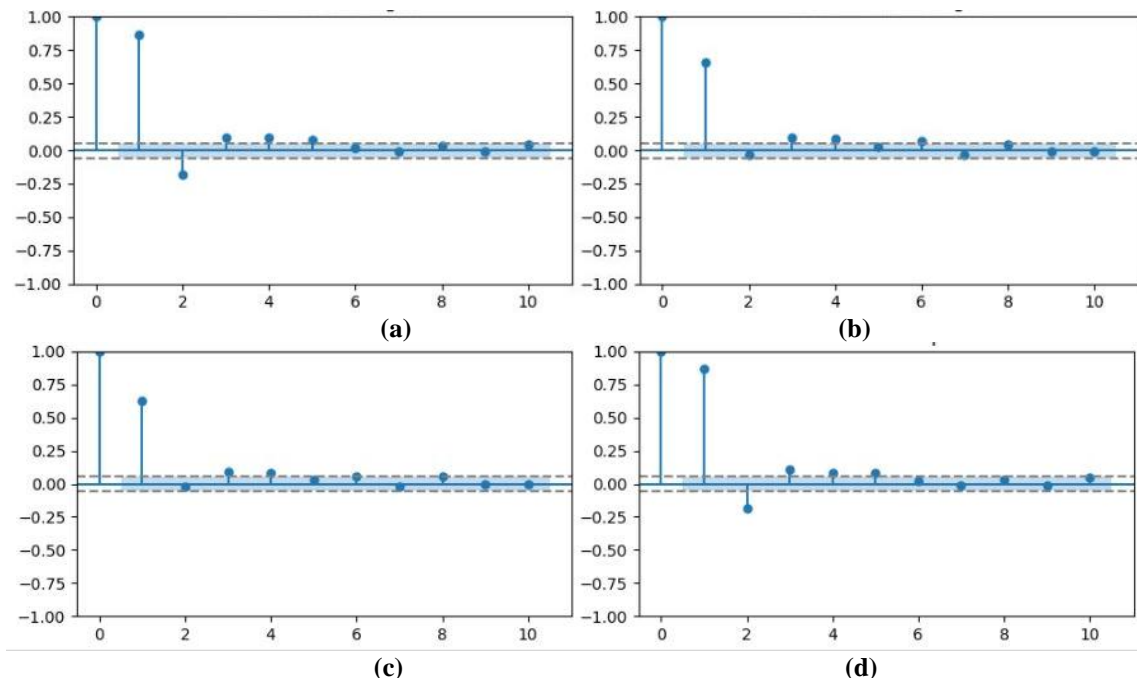


**Figure 4. Plot of PACF, (a) Wave Height PACF, (b) Wave Length PACF, (c) Wave Period PACF, (d) Wave Amplitude PACF.**

Then, the determination of sequential input data was carried out with the PACF plot for each variable as shown in **Figure 4**. This was done because each variable has its own data pattern. The PACF plot in this study uses a maximum lag limit of 10, and the significant lags will be used as sequential input data. The significant lags on the PACF plot for the height variable are lag 1, lag 2, lag 3, lag 4, and lag 5. For the length variable, the significant lags on the PACF plot are lag 1, lag 2, lag 3, lag 4, lag 5, and lag 6. For the period

variable, the significant lags on the PACF plot are lag 1, lag 2, lag 3, lag 4, lag 5, lag 6, lag 7, and lag 8. For the amplitude variable, the significant lags on the PACF plot are lag 1, lag 2, lag 3, lag 4, and lag 5. This lag is then used as time steps or time series patterns.

### 3.2 Result of Normalization and Time Series Patterns

The next step is min-max normalization for the variables of height, length, period, and wave amplitude to ensure that variables with excessively large ranges do not dominate the training and testing processes. Next, a sequential time series pattern is created based on the normalization results in **Table 5**. The time series pattern in **Table 6** is adjusted according to the lag values of each variable resulting from the PACF plot to produce three outputs, which are the one-day-ahead predictions for each variable. The dataset is divided into 80% for training and 20% for testing, resulting in 982 training data points from January 1st, 2021, to September 9th, 2023, and 240 testing data points from September 10th, 2023, to May 5th, 2024.

**Table 5. Normalization Dataset Result**

Date time	Wave height (m)	Wave period (s)	Wave length (m)	Wave amplitude (m)
2021-01-01	0.290424	0.478736	0.326604	0.289473
2021-01-02	0.279435	0.348724	0.215280	0.279904
2021-01-03	0.241758	0.414338	0.272674	0.240403
:	:	:	:	:
2024-05-05	0.177394	0.183475	0.090916	0.224880

**Table 6. Time Series Pattern**

Wave height	Wave height target	Wave length	Wave length target
$H_1, H_2, \dots, H_5$	$H_6$	$L_1, L_2, \dots, L_6$	$L_7$
$H_2, H_3, \dots, H_6$	$H_7$	$L_2, L_3, \dots, L_7$	$L_8$
:	:	:	:
$H_{1217}, H_{1218}, \dots, H_{1221}$	$H_{1222}$	$L_{1226}, L_{1227}, \dots, L_{1221}$	$L_{1222}$
Wave period	Wave period target	Wave amplitude	Wave amplitude target
$P_1, P_2, \dots, P_8$	$P_9$	$A_1, A_2, \dots, A_5$	$A_6$
$P_2, P_3, \dots, P_9$	$P_{10}$	$A_2, A_3, \dots, A_6$	$A_7$
:	:	:	:
$P_{1214}, P_{1215}, \dots, P_{221}$	$P_{1222}$	$A_{1217}, A_{1218}, \dots, A_{1221}$	$A_{1222}$

The time series patterns in **Table 6** different for each variable. For the height and amplitude variables, data from the 1st to the 5th is used as input, and the target data starts from the 6th data point. For the length variable, data from the 1st to the 6th is used as input, and the target length data starts from the 7th data point. For the period variable, data from the 1st to the 8th is used as input, and the target period data starts from the 9th data point.

### 3.3 Result of Hyperparameter Testing for Wave Height, Period, Length, and Amplitude

The LSTM model in this study uses the Adam function as its optimizer and the tanh function as its activation function. The hyperparameters of the LSTM algorithm include the number of neurons per layer, the number of epochs, and the batch size [37]. The situation where all inputs for the model pass through the entire neural network at once is called an epoch [38]. The number of data samples required by the model at each training iteration is known as the batch size; determining the batch size will affect the accuracy of the model. A neural network unit is the number of neurons or nodes in the hidden layer; determining the right amount allows the model more accurate, and reduce the complexity of the neural network [39].

This research uses hyperparameter testing as shown in **Table 7**. Based on **Table 7**, the MAPE values tend to be lower at epoch 50, with batch sizes of 32 and 64. These low MAPE values indicate good prediction accuracy, as visualized in the graph in **Figure 5**. The smallest MAPE value for the wave height is found at

50 neurons, 100 epochs, and a batch size of 64, amounting to 0.3657%. The smallest MAPE value for the wave length is found at 100 neurons, 50 epochs, and a batch size of 32, amounting to 0.1637%. The smallest MAPE value for the wave period is found at 50 neurons, 50 epochs, and a batch size of 32, amounting to 0.0888%. Additionally, the smallest MAPE value for the amplitude is found at 100 neurons, 50 epochs, and a batch size of 64, amounting to 0.3480%. A comparison graph of the actual and predicted data for each research variable is shown in **Figure 5**.

**Table 7. Result MAPE Value**

Neuron	Epoch	Batch Size	MAPE wave height (%)	MAPE wave length (%)	MAPE wave period (%)	MAPE wave amplitude (%)
50	50	16	0.4197	0.1698	0.0896	0.6933
		32	0.3795	0.1677	<b>0.0888</b>	0.3526
		64	0.4448	0.1996	0.0908	0.4692
	100	16	0.5148	0.2029	0.0995	0.5823
		32	0.6666	0.2031	0.964	0.7630
		64	<b>0.3667</b>	0.1721	0.0922	0.6714
100	50	16	0.3689	0.1766	0.0904	0.4340
		32	0.4620	<b>0.1637</b>	0.0920	0.4754
		64	0.3984	0.2028	0.0908	<b>0.3480</b>
	100	16	0.6109	0.1923	0.0924	0.4863
		32	0.6258	0.1889	0.0930	0.5950
		64	0.6580	0.1694	0.0954	0.4930

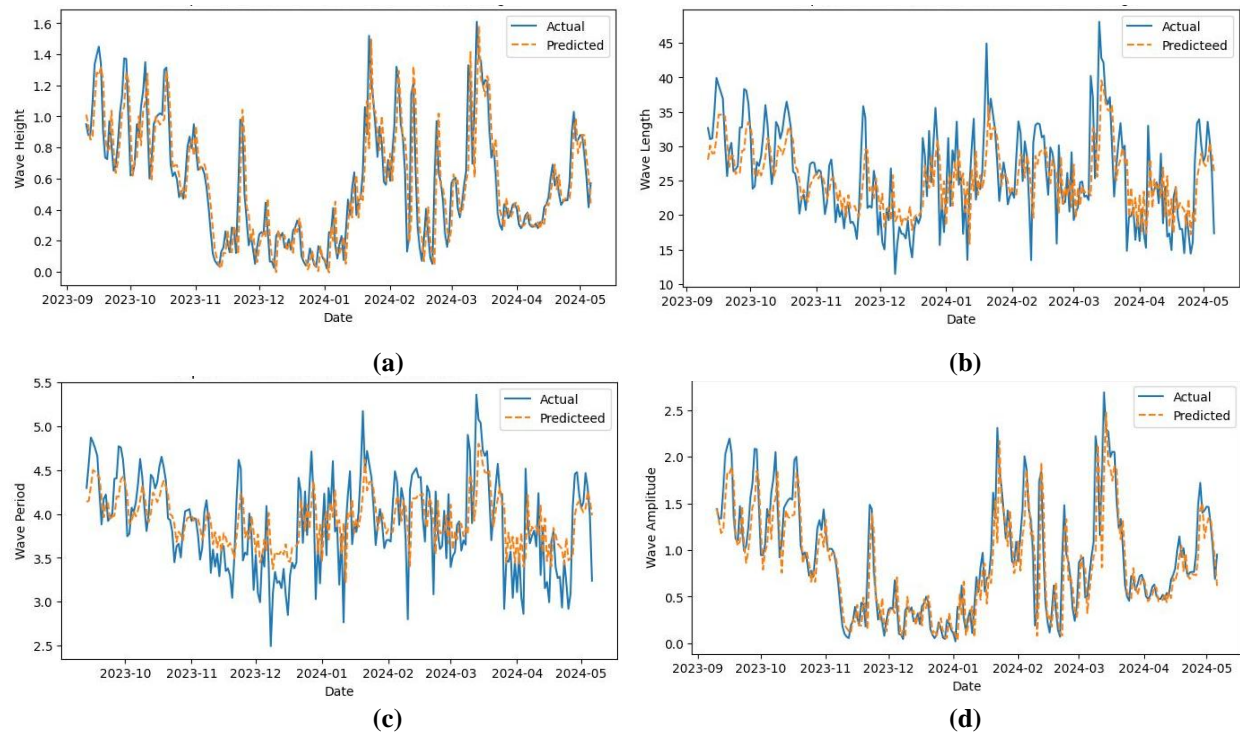


**Figure 5. Plot of Predicted Variable Results, (a) Wave Height Predicted, (b) Wave Length Predicted, (c) Wave Period Predicted, (d) Wave Amplitude Predicted.**

Based on **Figure 5**, The orange line representing the predicted values has followed the pattern or trend of the actual data on blue line, indicating that the training process has achieved an optimal model result. The range of predicted values for the height and wave amplitude variables nearly matches the range of their actual values, so the difference between the actual values and the predictions is relatively small. For the wave height, the actual value range is 0.02–1.61 meters, while the predicted value range is 0.004–1.584 meters. For the

wave amplitude, the actual value range is 0.02–2.69 meters, while the predicted value range is 0.03–2.47 meters. However, for the wave length and period, the range of predicted values is smaller than that of the actual values. Even though the model has recognized the patterns, the predicted values generated have not been able to follow the fluctuations of the plot as well as the predicted plots for wave height and wave amplitude. For example, in the plot of predicted wave period from 12-2023 to 01-2024, there is a tendency for the values to rise, while the actual plot shows a decline. For the wave length, the actual value range is 11.44–48.07 meters, while the predicted value range is 15.83–39.56 meters. For the wave period, the actual value range is 2.49–5.35 seconds, while the predicted value range is 3.22–4.79 seconds. Next, the prediction results for each variable with the lowest MAPE will be denormalized to their actual values and stored for use in predicting the electricity output of the OWC power plant.

### 3.4 Electricity Demand Prediction Results

The forecasting of electrical power was conducted using the predicted results from the testing data of each variable from September 13th, 2023, to May 5th, 2024 (237 data points). This number differs from the previous testing data due to adjustments in the predicted results caused by varying timesteps for each variable. The calculation of the large electric power of the OWC is carried out using the predicted results of each variable with the formula in Equation 1 by taking the chamber area of the OWC is 35m<sup>2</sup>. Then, the predicted electric power is compared with the actual electric power, resulting in a MAPE value of 0.3549%. The results of the actual and predicted electric power are presented in **Table 8** and **Table 9**.

**Table 8. Actual Electric Power**

Date time	Wave height (m)	Wave period (s)	Wave length (m)	Wave amplitude (m)	Actual power (Watt)
2023-09-13	1.085	4.295	31.160	1.645	723531.8700
2023-09-14	1.335	4.575	34.965	2.025	938263.7642
2023-09-15	1.395	4.870	39.935	2.115	1051459.579
:	:	:	:	:	:
2024-05-05	0.570	3.240	17.350	0.950	308415.0458

**Table 9. Predicted Electric Power**

Date time	Wave height (m)	Wave period (s)	Wave length (m)	Wave amplitude (m)	Actual power (Watt)
2023-09-13	0.858696	4.137172	28.96375	1.20628	511986.1912
2023-09-14	1.094180	4.149190	28.97151	1.54993	656113.4795
2023-09-15	1.283122	4.313828	31.22973	1.83950	807352.4270
:	:	:	:	:	:
2024-05-05	0.439983	3.983747	26.35007	0.61566	246883.1847

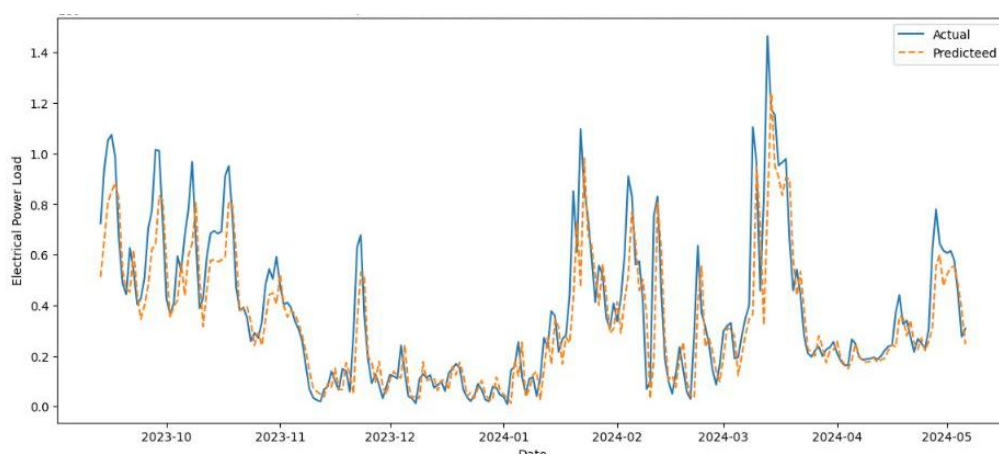


**Figure 6. Plot of Prediction Electric Power**

In the graph shown in **Figure 6**, the comparison of actual data and predicted electrical power indicates that the actual data, represented by the blue plot, and the predicted data, represented by the orange plot, show that the predicted plot follows the pattern or trend of the actual data. This suggests that the LSTM prediction model has good results and is close to the actual values. However, there is a difference between the actual value range and the predicted value. In actual values, the lowest electrical power occurred on January 2nd, 2024, at 8936.2142 Watts, and the highest electrical power occurred on March 13th, 2024, at 1464169.049 Watts. Meanwhile, in predicted values, the lowest electrical power occurred on January 3rd, 2024, at 12796.7271 Watts, and the highest electrical power occurred on March 14th, 2024, at 1238466.378 Watts. This difference in range indicates that the maximum predicted value cannot reach the actual maximum value, and the minimum predicted value exceeds the actual minimum value, both locally and globally. For example, on the date in question, the actual highest electrical power was 1464169.049 Watts, while the predicted value was 789456.1499 Watts. The difference is caused by the predicted values of the variables, particularly the wave length and wave period, which have a smaller range of predicted values, thus significantly affecting the results of the electrical power prediction.

#### 4. CONCLUSION

From the research results, it was concluded that the prediction of the amount of electrical power produced by PLTGL-OWC uses the method Long Short Term Memory (LSTM) with several trials hyperparameter such as neuron, epoch, and batch size produces a predicted value of electrical power with a MAPE of 0.3549%. The electric power prediction results are obtained through the predicted value of each variable with the lowest MAPE value. The smallest MAPE value for the wave height, length, period, and amplitude are 0.3657%, 0.1637%, 0.0888%, 0.3480%. This forecast is said to be very good because it has a MAPE value  $< 10\%$ . Based on this, this model can be used as a tool to provide more accurate prediction results to support more efficiency and minimize problems when distributing electrical energy.

#### AUTHOR CONTRIBUTIONS

Risma Madurahma Putri: Conceptualization, Data curation, Formal analysis, Investigation, Methodology, Visualization, Writing - original draft. Luthfi Hakim: Funding acquisition, Project administration, Resources, Supervision, Validation, Visualization, Writing - review and editing. Dian C Rini Novitasari: Funding acquisition, Validation, Writing - review and editing, Ahmad Hanif Asyhar: Funding acquisition, Validation, Writing - review and editing. Fajar Setiawan: Data curation, Validation, Writing - review & editing. All authors discussed the results and contributed to the final manuscript.

#### FUNDING STATEMENT

This research received no funding from any public agency.

#### ACKNOWLEDGMENT

Thank you to Perak Maritime Meteorology Station II, Surabaya, for providing the sea wave data that made this research possible.

#### CONFLICT OF INTEREST

The authors declare no conflicts of interest to report study.

## REFERENCES

- [1] J. U. Jasron, D. P. Mangesa, K. Boimau, B. V. Tarigan, E. U. K. Maliwemu, and M. Salombe, "ANALISA POTENSI GELOMBANG LAUT SEBAGAI SUMBER ENERGI TERBARUKAN MENGGUNAKAN PERANGKAT OSCILLATING WATER COLUMN (OWC) DI WILAYAH PERAIRAN LAUT TIMOR," *LONTAR J. Tek. Mesin Undana*, vol. 9, no. 01, pp. 14–20, 2022, doi: <https://doi.org/10.35508/ljtmu.v9i01.7269>.
- [2] S. Nengsih, "POTENSI AIR LAUT ACEH SEBAGAI SUMBER ENERGI LISTRIK ALTERNATIF," *CIRCUIT J. Ilm. Pendidik. Tek. Elektro*, vol. 4, no. 2, p. 81, 2020, doi: <https://doi.org/10.22373/crc.v4i2.6496>.
- [3] A. Vidura, R. L. W, and Mukhtasor, "POTENSI PEMANFAATAN PEMBANGKIT LISTRIK TENAGA GELOMBANG LAUT DI PERAIRAN SELATAN PULAU JAWA DALAM MENDUKUNG KETAHANAN ENERGI," *J. Ketahanan Energi*, vol. 8, no. 1, pp. 32–48, 2022.
- [4] A. Rohman and H. Yuliandoko, "STUDI KARAKTERISTIK PEMBANGKIT LISTRIK TENAGA GELOMBANG AIR LAUT (PLTGL) SEBAGAI ENERGI TERBARUKAN," *Semin. Nas. Terap. Ris. Inov. Ke-6*, vol. 6, no. 1, pp. 129–137, 2020.
- [5] B. Y. Suprapto, "DESAIN PENGEMBANGAN SISTEM PEMBANGKIT LISTRIK TENAGA GELOMBANG LAUT BERBASIS KESEIMBANGAN GYROSCOPE," *J. Surya Energy*, vol. 5, no. 2, pp. 50–54, 2022, doi: <https://doi.org/10.32502/jse.v5i2.3328>.
- [6] S. Setiyawan and N. Abdulrahim, "PEMBANGKIT LISTRIK TENAGA GELOMBANG LAUT DENGAN MENGGUNAKAN TEKNOLOGI OSCILATING WATER COLUMN (OWC) DI PERAIRAN MARANA," *REKONSTRUKSI TADULAKO Civ. Eng. J. Res. Dev.*, pp. 59–68, 2021, doi: <https://doi.org/10.22487/renstra.v2i1.224>.
- [7] D. K. Sari and S. Fahrezy, "Pengaruh Angin Terhadap Karakteristik Gelombang Laut Di Pulau SAUGI Kabupaten Pangkajene dan Kepulauan," *Indones. J. Geogr.*, vol. 1, no. 1, pp. 11–19, 2023, [Online]. doi: <https://doi.org/10.26858/ijag>
- [8] N. H. Sarira and P. R. Pong-Masak, "SEAWEED SELECTION TO SUPPLY SUPERIOR SEEDS FOR CULTIVATION," *J. Perikan. Univ. Gadjah Mada*, vol. 20, no. 2, p. 79, 2019, doi: <https://doi.org/10.22146/jps.36109>.
- [9] T. R. Yudisthira, "ANALISIS DAN IMPLEMENTASI ALGORITMA PEMANTAUAN KUALITAS ENERGI LISTRIK PADA SISTEM SMART GRID," *Cosm. J. Tek.*, vol. 1, no. 4, pp. 165–174, 2024.
- [10] B. Y. Phiadelvira, D. Z. Haq, D. C. R. Novitasari, and F. Setiawan, "PREDIKSI BESAR DAYA LISTRIK TENAGA GELOMBANG LAUT METODE OSCILLATING WATER COLOUMN (PLTGL-OWC) DI BANYUWANGI MENGGUNAKAN EXTREME LEARNING MACHINE (ELM)," *Unnes J. Math.*, vol. 11, no. 1, pp. 1–7, 2022, doi: <https://doi.org/10.15294/ujm.v1i11.50967>.
- [11] C. Gu and H. Li, "REVIEW ON DEEP LEARNING RESEARCH AND APPLICATIONS IN WIND AND WAVE ENERGY," *Energies*, vol. 15, no. 4, 2022, doi: <https://doi.org/10.3390/en15041510>.
- [12] S. Poornima and M. Pushpalatha, "PREDICTION OF RAINFALL USING INTENSIFIED LSTM BASED RECURRENT NEURAL NETWORK WITH WEIGHTED LINEAR UNITS," *Atmosphere (Basel.)*, vol. 10, no. 11, 2019, doi: <https://doi.org/10.3390/atmos10110668>.
- [13] M. Musfiroh, D. C. R. Novitasari, P. K. Intan, and G. G. Wisnawa, "PENERAPAN METODE PRINCIPAL COMPONENT ANALYSIS (PCA) DAN LONG SHORT TERM MEMORY (LSTM) DALAM MEMPRIDIksi PREDIKSI CURAH HUJAN HARIAN," *Build. Informatics, Technol. Sci.*, vol. 5, no. 1, pp. 1–11, 2023, doi: <https://doi.org/10.47065/bits.v5i1.3114>.
- [14] M. Rajendar, D. M. Reddy, M. Nagesh, and V. Nagaraju, "PROGRESSION OF COVID-19 CASES IN TELANGANA STATE BY USING ARIMA, MLP, ELM AND LSTM PREDICTION MODELS BY RETROSPECTIVE CONFIRMATION," *Indian J. Sci. Technol.*, vol. 17, no. 12, pp. 1159–1166, 2024, doi: <https://doi.org/10.17485/IJST/v17i12.211>.
- [15] "Bawean Island," 2024. [https://www.google.com/maps/place/Pulau+Bawean/@5.7933274,112.5732551,12z/data=!3m1!4b1!4m6!3m5!1s0x2ddf5782884529d1:0x52621acdfb67b026!8m2!3d5.787058!4d12.6619386!16zL20vMDZwYjZ?entry=ttu&g\\_ep=EgoyMDI0MTAyMy4wIKXMDSoASAFQAw%3D%3D](https://www.google.com/maps/place/Pulau+Bawean/@5.7933274,112.5732551,12z/data=!3m1!4b1!4m6!3m5!1s0x2ddf5782884529d1:0x52621acdfb67b026!8m2!3d5.787058!4d12.6619386!16zL20vMDZwYjZ?entry=ttu&g_ep=EgoyMDI0MTAyMy4wIKXMDSoASAFQAw%3D%3D)
- [16] M. Zulhaidir and M. Arman, "ANALISIS KEAMANAN DAN STABILITAS BANGUNAN PESISIR TERHADAP HANTAMAN GELOMBANG DI PANTAI MERPATI, KAB. BULUKUMBA," *Arus J. Sains dan Teknol. ( AJST )*, vol. 2, no. 1, 2024. doi: <https://doi.org/10.57250/ajst.v2i1.336>
- [17] P. R. F. Teixeira and E. Didier, "NUMERICAL ANALYSIS OF THE RESPONSE OF AN ONSHORE OSCILLATING WATER COLUMN WAVE ENERGY CONVERTER TO RANDOM WAVES," *Energy*, vol. 220, p. 119719, 2021, doi: <https://doi.org/10.1016/j.energy.2020.119719>.
- [18] S. Arrohman and D. A. Himawanto, "PELUANG PELUANG DAN TANTANGAN PENGEMBANGAN TEKNOLOGI OSCILATING WATER COLUMN (OWS) DI INDONESIA.," *J. Energi dan Teknol. Manufaktur*, vol. 4, no. 01, pp. 37–42, 2021, doi: <https://doi.org/10.33795/jetm.v4i01.24>.
- [19] F. Y. Nagifea, "POTENSI PEMBANGKIT LISTRIK TENAGA GELOMBANG LAUT (PLTGL) SEBAGAI ENERGI ALTERNATIF DI INDONESIA," *J. Technopreneur*, vol. 10, no. 2, pp. 17–24, 2022, doi: <https://doi.org/10.30869/jtech.v10i2.968>.
- [20] D. Mahroni. Supriyatna, "ENERGI BARU TERBARUKAN DALAM PEMBANGUNAN YANG BERKELANJUTAN DAN PEMANFAATAN ENERGI TERBARUKAN," *Kohesi J. Multidisiplin Saintek*, vol. 2, no. 11, pp. 66–76, 2024.
- [21] C. A. Siregar and S. Lubis, "PERENCANAAN INSTRUMEN KONVERSI ENERGI TENAGA GELOMBANG DENGAN MENGGUNAKAN TEKNIK KOLOM OSILASI," *J. MESIL (Mesin Elektro Sipil)*, vol. 1, no. 1, pp. 63–71, 2020, doi: <https://doi.org/10.53695/jm.v1i1.156>.
- [22] S. Rohmaniatul, A. F. Pratiwi, and S. Rahmat, "RANCANG BANGUN PEMBANGKIT LISTRIK TENAGA GELOMBANG LAUT MENGGUNAKAN SISTEM OSCILLATING WATER COLUMN," *Infotekmesin*, vol. 12, no. 1, pp. 42–49, 2021, doi: <https://doi.org/10.35970/infotekmesin.v12i1.412>.
- [23] L. N. Nur Afifah and I. T. Safira, "OPTIMALISASI DESAIN TURBIN WELLS PADA SISTEM OSILASI KOLOM AIR PEMBANGKIT LISTRIK TENAGA GELOMBANG LAUT SEBAGAI UPAYA MENINGKATKAN POTENSI SUPPLY ENERGI TERBARUKAN PADA MASYARAKAT PESISIR," *J. Offshore Oil, Prod. Facil. Renew. Energy*, vol. 4, no. 2, pp. 26–37, 2020, doi: <https://doi.org/10.30588/jo.v4i2.831>.
- [24] M. T. A. Firdaus, M. Syaukani, A. S. Irfan, A. P. M. Jaya, and R. Yanuar, "STUDI KELAYAKAN POTENSI PEMBANGKIT LISTRIK GELOMBANG LAUT OSCILLATING WATER COLUMN (PLTGL-OWC) DI PERAIRAN PESISIR BARAT LAMPUNG," *Proceeding Technol. Renew. Energy Dev. Conf. 2*, vol. 3, no. 1, pp. 21–30, 2023.

[25] I. Gede *et al.*, "IMPLEMENTASI METODE ANALYTICAL HIERARCHY PROCESS DAN INTERPOLASI LINIER DALAM PENENTUAN LOKASI WISATA DI KABUPATEN KARANGASEM," *J-SAKTI (Jurnal Sains Komput. dan Inform.,*, vol. 5, no. 2, pp. 866–878, 2021, [Online]. Available: <https://www.tunasbangsa.ac.id/ejurnal/index.php/jsakti/article/view/383>

[26] M. N. Fadilah, A. Yusuf, and N. Huda, "PREDIKSI BEBAN LISTRIK DI KOTA BANJARBARU MENGGUNAKAN JARINGAN SYARAF TIRUAN BACKPROPAGATION," *J. Mat. Murni Dan Terap. Epsil.*, vol. 14, no. 2, p. 81, 2021, doi: <https://doi.org/10.20527/epsilon.v14i2.2961>.

[27] S. Zahara and S. Sugianto, "PREDIKSI INDEKS HARGA KONSUMEN KOMODITAS MAKANAN BERBASIS CLOUD COMPUTING MENGGUNAKAN MULTILAYER PERCEPTRON," *JOINTECS (Journal Inf. Technol. Comput. Sci.,* vol. 6, no. 1, p. 21, 2021, doi: <https://doi.org/10.31328/jointecs.v6i1.1702>.

[28] F. T. Admojo and Y. I. Sulisty, "ANALISIS PERFORMA ALGORITMA STOCHASTIC GRADIENT DESCENT (SGD) DALAM MENKLASIFIKASI TAHU BERFORMALIN," *Indones. J. Data Sci.,* vol. 3, no. 1, pp. 1–8, 2022, doi: <https://doi.org/10.56705/ijodas.v3i1.42>.

[29] A. Winata, M. Dolok Lauro, and T. Handhayani, "PERBANDINGAN LSTM DAN ELM DALAM MEMPREDIKSI HARGA PANGAN KOTA TASIKMALAYA," *J. Ilmu Komput. dan Sist. Inf.,* vol. 11, no. 2, 2023, doi: <https://doi.org/10.24912/jiksi.v11i2.26015>.

[30] J. Jtik, J. Teknologi, F. Kurnia, T. Putri, and A. D. Wowor, "IMPLEMENTASI ALGORITMA LONG SHORT TERM MEMORY DALAM PREDIKSI KONSENTRASI GAS METANA ( CH4 ) DI KOTA SALATIGA," vol. 8, no. 2, 2024.doi: <https://doi.org/10.35870/jtik.v8i2.1917>

[31] R. Anik and E. M. Afif, "ANALISIS TIME SERIES UNTUK MENENTUKAN MODEL TERBAIK PRODUK SONGKOK NASIONAL DI KABUPATEN GRESIK," *Pros. Semin. Nas. Mat. dan Ter.,* pp. 1–16, 2018.

[32] S. Vincentius Riandaru Prasetyo\*, Stefan Axel, Juan Timothy Soebroto, David Sugiarto and S. D. N. Ardi Winatan, "PREDIKSI HARGA EMAS BERDASARKAN DATA GOLD.ORG MENGGUNAKAN METODE LONG SHORT TERM MEMORY," *Sist. J. Sist. Inf.,* vol. 11, pp. 623–629, 2022.doi: <https://doi.org/10.32520/stmsi.v11i3.1999>

[33] D. Z. Haq *et al.*, "LONG SHORT TERM MEMORY ALGORITHM FOR RAINFALL PREDICTION BASED ON EL-NINO AND IOD DATA," *Procedia Comput. Sci.,* vol. 179, no. 2019, pp. 829–837, 2021, doi: <https://doi.org/10.1016/j.procs.2021.01.071>.

[34] D. D. Pramesti, D. C. R. Novitasari, F. Setiawan, and H. Khaulasari, "LONG-SHORT TERM MEMORY (LSTM) FOR PREDICTING VELOCITY AND DIRECTION SEA SURFACE CURRENT ON BALI STRAIT," *BAREKENG J. Ilmu Mat. dan Terap.,* vol. 16, no. 2, pp. 451–462, 2022, doi: <https://doi.org/10.30598/barekengvol16iss2pp451-462>.

[35] A. Y. Labolo *et al.*, "COMPARASI ALGORITMA FORECASTING SVM , K-NN DAN NN," *J. Sci. Soc. Res.,* vol. 4307, no. 2, pp. 289–299, 2022, [Online]. Available: <http://jurnal.goretanpena.com/index.php/JSSR>

[36] I. I. Zulfa, D. C. R. Novitasari, F. Setiawan, A. Fanani, and M. Hafiyusholeh, "PREDICTION OF SEA SURFACE CURRENT VELOCITY AND DIRECTION USING LSTM," *IJEIS (Indonesian J. Electron. Instrum. Syst.,* vol. 11, no. 1, p. 93, 2021, doi: <https://doi.org/10.22146/ijeis.63669>.

[37] N. Ananda, H. S. Wicaksana, Y. G. Wijaya, and R. Hijazi, "HYPERPARAMETER TUNING LSTM SEBAGAI ESTIMATOR SENSOR RELATIVE HUMIDITY PADA AUTOMATIC WEATHER STATION BERBASIS SIMULATED ANNEALING," *Bul. Meteorol. Klimatologi, Dan Geofis.,* vol. 4, no. 1, pp. 35–43, 2023.

[38] F. Nashrullah, S. A. Wibowo, and G. Budiman, "Investigasi Parameter Epoch Pada Arsitektur ResNet-50 Untuk Klasifikasi Pornografi," *J. Comput. Electron. Telecommun.,* vol. 1, no. 1, pp. 1–8, 2020, [Online]. Available: <https://scholar.archive.org/work/5rwpasnveze2lj76wgj62lxaya/access/wayback/https://jurnal.itelkom-sby.ac.id/complete/article/download/51/53>

[39] M. A. Rohman, Suhartono, and T. Chamidy, "BIDIRECTIONAL GRU DENGAN ATTENTION MECHANISM PADA ANALISIS SENTIMEN PLN MOBILE BIDIRECTIONAL GRU WITH ATTENTION MECHANISM ON SENTIMENT ANALYSIS OF PLN MOBILE," *Techno.com,* vol. 22, no. 2, pp. 358–372, 2023.doi: <https://doi.org/10.33633/tc.v22i2.7876>

